JOURNAL OF MATERIALS SCIENCE 23 (1988) 3338–3341

On the effect of non-metallic inclusions on hydrogen damage in aluminium-killed steel

ESTELA RODRÍGUEZ de SCHIAPPARELLI
Departamento Materiales, Gerencia Desarrollo, Comision Nacional de Energía Atómica, Av. del Libertador 8250, 1429 Buenos Aires, Argentina

The effect of non-metallic inclusions on corrosion and on hydrogen damage in an aluminium-killed steel was studied by considering the size, shape, composition and number of inclusions. Accurate determinations of the compositions of the different inclusion compounds were performed by energy-dispersive analysis of replica-extracted particles. Clusters of alumina inclusions appear to be preferred sites for the occurrence of blisters. Complex inclusions with the phases $3Al_2O_3 \cdot 2SiO_2$, MnO, MnS and Al_2O_3 frequently presented blisters. Blisters appeared to be nucleated in voids produced during working of the steel. Blisters were never found in MnS inclusions.

1. Introduction

The effect of non-metallic inclusions on corrosion processes in carbon steel is generally accepted [1, 2] to be related to the more noble nature of MnS and FeS with respect to the ferritic matrix. They might therefore act as local cathodes inducing oxidation of iron, mainly at the inclusion–matrix interfaces. Polarization and concentration of aggressive anions such as chlorides might occur in the microcrevices thus generated. Sulphides dissolved in neutral and acid media producing cations may eventually hydrolyse, thus contributing to a rise of acidity within the micropits.

Hydrogen-induced damage may also be related to inclusions. In mild steel a hydrogen charge produces internal crevices and blisters. These blisters initiate at internal interfaces at which hydrogen is evolved in gaseous form. The evolution of hydrogen is easy at interfaces featuring a low coherence between the matrix and the inclusion, which may even be separated by microvoids. This model was widely accepted by Szklarska-Smialowska and Lunarska [3].

In high-strength steel, atomic hydrogen concentrates in the highly stressed regions, giving rise to decohesion of the crystal lattice and failure by crack propagation. This model was proposed by Oriani [4].

There are several opinions concerning the type of inclusions which produce hydrogen damage. Among the most important is the point of view of Ciszewski [5] about the difference in tessellated stresses, generated during quenching around some inclusions (mainly oxides) in tempered steel, caused by the low thermal coefficient compared with that of the matrix.

Szklarska-Smialowska and Lunarska [3] analysed the type of matrix–inclusion bonding in low-carbon steel. Silicates will be the inclusions which may initiate internal blistering, since they have the weakest type of bonding to the matrix.

Wilde *et al.* [6], Pressouyre *et al.* [7] and Yoichi *et al.* [8] have observed that the most advantageous sites for hydrogen damage initiation are the elongated MnS inclusions.

The difference in opinion may be partly due to the difficulties in characterizing the inclusions in steel. The limitations in the use of conventional and non-conventional techniques using light microscopy, energy-dispersive X-ray analysis (EDAX) and scanning electron microscopy, were studied by Schiapparelli *et al.* [9].

Monochromatic X-ray methods are of great value for inclusion studies as they give a very low background, and it is possible to study low-angle reflections. These reflections are of special importance for the identification of the complex X-ray powder photographs of inclusion phases, but it is not usually possible to carry out a phase analysis using the actual steel inclusions because they are frequently too small.

In the present work, a non-conventional technique of analysis is used. This technique allows one to characterize the phases present in the inclusions. According to the experimental data, an attempt is made to determine which types of inclusion are more liable to initiate hydrogen damage, and to provide some possible explanation of the phenomenon.

2. Experimental procedure

Specimens of aluminium-killed steel of chemical composition (wt %) C 0.14, S 0.006, Si 0.25, Al 0.05, Mn 1.11, Ca 0.005 and P 0.01 were used in the present work. Test specimens measuring 20 mm × 10 mm × 2 mm were extracted from the material as shown in Fig. 1.

2.1. Characterization of inclusions

The size, distribution, morphology, shape and number of the inclusions were studied by conventional light microscopy, quantitative microscopy and scanning electron microscopy (SEM), in the latter case etching

0022–2461/88 $03.00 + .12

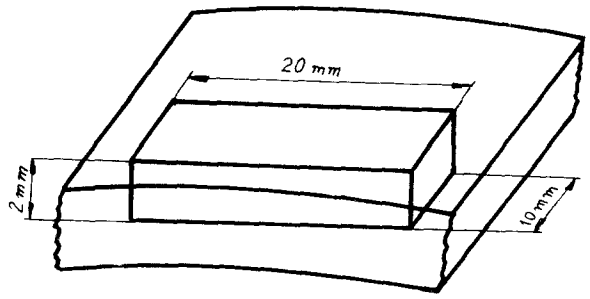

Figure 1 Extraction of test specimens.

with Br/CH_3OH solution. In order to study the chemical compositions of the phases that comprise the inclusions, a non-conventional technique [10] was used. Inclusions were removed from the matrix by epoxy replicas, etched with Br/CH_3OH solution and analysed by EDAX. The Br/CH_3OH solution was chosen in order to avoid the dissolution of the inclusion, given that the inclusion phases are more noble than the matrix, except for CaS. The same formalism of thin-foil analysis was used in our work. Stoichiometric calculations were possible due to the absence of matrix effects.

The specimens were polished with 0.25 μm diamond paste and cathodically charged, using several electrolytes (Table 1) in order to obtain different concentrations of the species S^{2-}, HS^- and H_2S based on the chemical solubility of MnS, in different pH solutions [11].

Other specimens were immersed in NACE solution consisting of an H_2S acid-saturated solution containing 0.5% acetic acid + 5% NaCl having a pH of 3.5. The experiments are listed in Table I.

3. Results

SEM observations of specimens etched with Br/CH_3OH solution show that inclusions are segregated between pearlite bands. The morphology and size of the inclusions are shown in Figs 2, 3 and 4. The types of inclusion are listed in Table II.

The Type 3 inclusion (Table II) comprised of MnS, Al_2O_3, MnO and $3Al_2O_3 \cdot 2SiO_2$ could be confused with MnS of Type II in the classification given by Sims and Dahle [12], when a qualitative EDAX analysis is made. On the other hand, if it is possible to know which phases are present, and the ratio of each phase, the Type 3 inclusion is identified as mainly mullite.

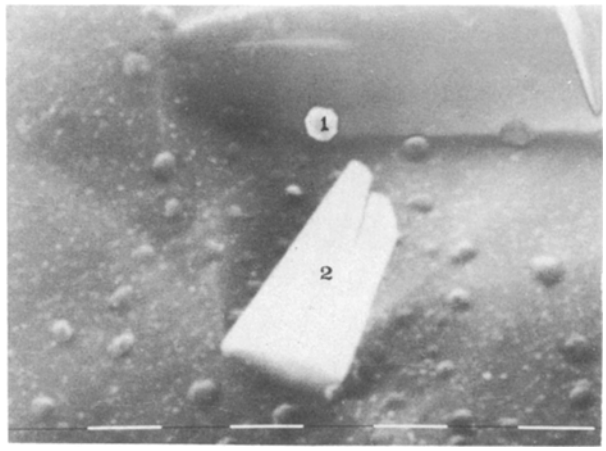

Figure 2 SEM micrograph of specimen. Morphology of alumina inclusions: numerals indicate Type 1 and Type 2 (Table II). Scale bars 10 μm.

In Type 3 and 4 inclusions, the different shapes are rather related to size, and not to chemical composition. The size of the inclusion depends on the solidification parameters.

The absence of FeS in all the inclusions is indicative that the cooling rate was low. This is concluded because MnS is thermodynamically more stable than FeS at low temperature. Our observations are not consistent with those of Wràglen [1] who reported that for low cooling rates a fine dispersion of submicroscopic inclusion should not be present.

According to Kiessling and Lange [13] the presence of mullite together with Al_2O_3 and MnO is frequent in hot-worked steel as well as endogenous inclusions. By means of light microscopy the SiO_2 phase cannot be differentiated from the mullite phase, as they show the same optical properties.

Hydrogen damage in galvanostatically charged specimens, and specimens immersed in NACE solutions, is summarized in Table III. Blisters were observed in all cases at matrix–alumina particle interfaces, independent of their size and shape. Large inclusions, comprised principally of mullite, frequently present blisters at the matrix–inclusion interface, whilst for small and spherical ones blisters were never found. Blisters were never found in MnS inclusions (Type II of Sims and Dahle [12]). Blisters of galvanostatically hydrogen charged specimens had a small size compared with those specimens immersed in NACE solution.

TABLE I Experimental conditions

Experiment No.	Electrolyte	Hydrogen promoter	Cathodic current density ($A\,m^{-2}$)	Cathodic charge time (sec)
1	0.1 N NaOH	0.08 N KCN	2.5×10^{-4}	2640
2	0.1 N NaOH	0.08 N KCN	2×10^{-3}	2640
3	0.1 N NaOH	–	2×10^{-3}	2640
4	0.1 N Na_2SO_4	13 p.p.m. As_2O_3	2×10^{-2}	2640
5	0.1 N Na_2SO_4	–	2×10^{-2}	2640
6	0.1 N H_2SO_4	13 p.p.m. As_2O_3	5×10^{-3}	2640
7	0.1 N H_2SO_4	–	5×10^{-3}	2640
8	NACE solution: H_2S satured solution containing 0.5% acetic acid + 5% NaCl, pH 3.5	–	–	3456×10^2

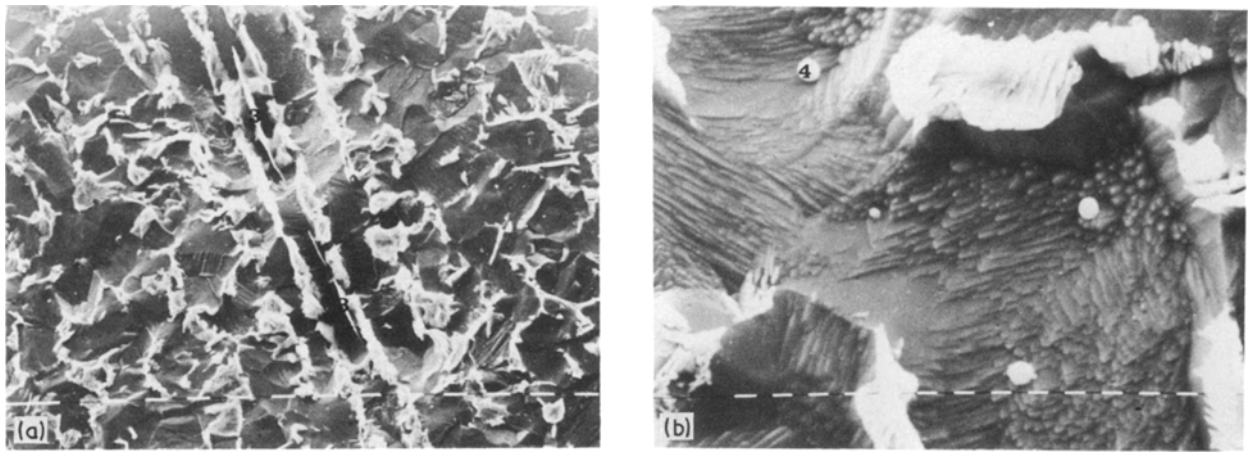

Figure 3 SEM micrograph of specimen. Morphology of complex inclusions: (a) Type 3, (b) Type 4. Scale bars 10 μm.

4. Discussion

For a better understanding of the phenomenon, the chemical and electrochemical reactions on the metal electrolyte surface are first considered.

4.1. Surface damage

In general during hot-working processing, variables such as temperature and strain are not effective in controlling inclusion plasticity. Voids are then produced between fractured fragments and/or at the ends of inclusions. In our material voids were found in large inclusions, at the interfaces of the same inclusions and at the ends of Al_2O_3 particles. In these voids a potential drop may happen due to H_2 gas evolution during cathodic charging.

In Experiments 4 to 7 the effects of promoters of hydrogen in acid and neutral aqueous solutions were compared. No differences were found in hydrogen damage when hydrogen promoters were used, because of the fact that sulphide inclusions in acid and neutral aqueous solutions are sources of the soluble species HS^-, S^{2-} and H_2S which are known to be powerful catalysts of electrochemical reactions [1]. It is also well known that sulphide ions inhibit the attainment of equilibrium between atomic and molecular hydrogen [14–16]. In addition the chemical dissolution of inclusions generates microvoids of different size and shape, according to the geometry of the inclusions and their relative orientation. At matrix–inclusion interfaces at right-angles to the rolling direction there occurs an intense corrosion that could be explained by considering the potential drop that may happen in the pits due to H_2 evolution. In spite of the cathodic polarization of the specimens this might produce oxidation of the matrix.

4.2. Bulk damage

Taking into account previous observations, damage caused by hydrogen in this material is related to inclusions. In all cases the observed damage consisted of internal microcavities associated with inclusions (blistering).

Not all types of inclusion presented blisters. The blisters were started at internal interfaces between the matrix and hard inclusions, principally alumina, which were not deformed plastically during hot-working at any temperature. Blisters were also found in large complex inclusions comprised of alumina, mullite, manganese oxide and manganese sulphide. In fact the presence of a hard undeformable phase such as alumina could act as a supporting framework which decreases the apparent plasticity of these inclusions. Inclusions of Type 5 which are deformed plastically during rolling never presented blisters at the matrix–inclusion interface. The same observations were made in other work [14]. However, Presouyre *et al.* [7] and Brown and Jones [15] observed that MnS Type II inclusions (according to the classification of Sims and Dahle [11]) were related to hydrogen damage. It is believed that this is a problem caused by the technique chosen for characterization of the inclusions.

Our observations are interpreted as follows. According to Bernard and Talbot [16] the hydrogen solubility is a function of the strain concentration. On the other hand the strain concentrations around inclusions depend upon the stress field around the inclusions. The magnitudes of the stresses up around an inclusion in a deformed steel depend principally upon the ratio of the plasticities of the inclusion and the matrix, as well as upon the shape, size, number and distribution of the inclusions. A deformed steel presents a high

TABLE II Characterization of the inclusions

Type	Inclusion phases (wt %)	Diameter range (μm)	Shape	Number of inclusions per m^2
1	100% Al_2O_3	1 to 4	Irregular	5.7×10^{10}
2	100% Al_2O_3	5 to 10	Irregular	1.5×10^{11}
3	10% Al_2O_3; 5% MnO; 5% MnS; 80% mullite	20 to 40	Elongated	1×10^{6}
4	As above	1 to 4	Spherical	1.1×10^{10}
5	95% MnS; 5% Al_2O_3	10 to 30	Elongated	7×10^{3}

TABLE III Experimental results

Experiment No.	Hydrogen damage (blistering)	Frequency of defects (percentage of inclusions that presented defect)	Surface damage
1	–	–	Not observed
2	Microcavities associated with Al_2O_3 inclusions	10	Not observed
3	–	–	Not observed
4	Microcavities associated with Al_2O_3 and complex inclusions (Type 3)	25	Not observed
5	As above	25	Not observed
6	As above	40	Dissolution of MnS inclusion
7	As above	40	As above
8	As above	50	Intense generalized corrosion

stress field around undeformable inclusions [13]. So the matrix that surrounds hard inclusions has a higher hydrogen saturation concentration, whereas the matrix surrounding soft inclusions has a low hydrogen saturation concentration. Thus the stress concentration around an inclusion and the charging conditions for hydrogen determine the hydrogen concentration in solid solution. This hydrogen concentration could be in equilibrium with gaseous H_2 inside the voids at matrix–inclusion interfaces. It is well known that voids are frequently nucleated at the ends of inclusions during rolling, especially if the inclusions have a non-plastic behaviour. Voids grow when the hydrogen pressure level is above strength for the steel.

5. Conclusions

1. Blisters were never found associated with soft inclusions, for example MnS.

2. Blisters associated with hard inclusions were always present independent of their size, for example Al_2O_3 inclusions.

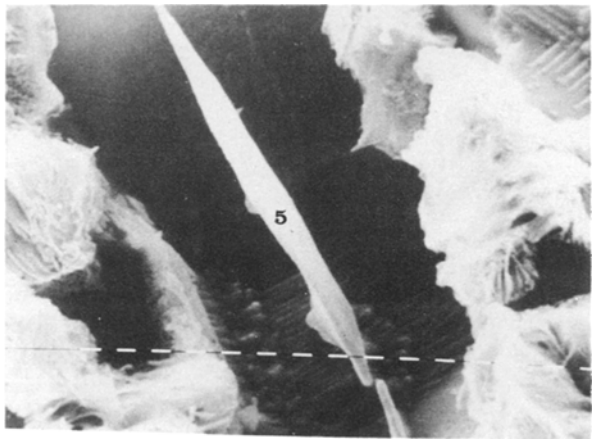

Figure 4 SEM micrograph of specimen. Morphology of MnS inclusions (Type 5). Scale bars 10 μm

3. Complex inclusions comprised of some hard phase frequently presented blisters. In this case the formation of blisters depends on their size.

Acknowledgements

The author would like to acknowledge the assistance of Dr Raul Versaci in the microanalysis of particles and Ing A. Hey and Dr M. Ipohorski for their contribution to this investigation.

References

1. G. WRÅNGLEN, *Corrosion Sci.* **14** (1974) 331.
2. H. PAMPHREY, *Corrosion* **36** (1980) 536.
3. Z. SZKLARSKA-SMIALOWSKA and E. LUNARSKA, *Korrosion* **32** (1981) 478.
4. R. ORIANI, *Ann. Rev. Mater. Sci.* **8** (1978) 327.
5. A. CIZEWSKI, Stress Corrosion Cracking and Hydrogen Embrittlement of Iron Base Alloys, NACE-5 (R. Staehle, T. Hochmann, R. Cright, T. Slater, eds.), NACE, Houston, Texas (1977) 671.
6. B. WILDE, C. KIM and E. PHELPS, *Corrosion* **36** (1980) 625.
7. G. PRESSOUYRE, R. BLONDEAU, G. PRIMON and L. GANDIOU, American Society for Metals, Metals Park, Ohio (1982) 212.
8. N. YOICHI, H. KURAHASHI, T. PMI and O. HIDA, *Trans. ISIJ* **19** (1979) 401.
9. E. SCHIAPPARELLI and A. HEY, *Mem. Sci. Rev. Metall.* (May 1984) 273.
10. E. R. SCHIAPPARELLI, *Non-Destructive Testing Commun.* **3** (1987) 39.
11. C. HUDGINS, R. GLASSON, P. MEHDIZADEH and P. ROBOSROUGH, *Corrosion* **22** (1966) 283.
12. C. SIMS, *Trans. AIME* **215** (1959) 367.
13. R. KIESLING and N. LANGE, "Non-metallic Inclusions in Steel", Part II, Publication 100 (Iron & Steel Institute, London, 1966).
14. E. SCHIAPPARELLI, *Materials Performance* **27** (1988) 21.
15. A. BROWS and C. JONES, *Corrosion* **40** (1984) (7).
16. S. BERNARD and J. TALBOT, *Compt. Rend.* **244** (1957) 1193.

Received 2 October 1987
and accepted 26 January 1988